



Clinical detection of Hepatitis C viral infection by yeast-secreted HCV-core:Gold-binding-peptide

A.G. Venkatesh^a, H. Brickner^b, D. Looney^{b,c}, D.A. Hall^a, E. Aronoff-Spencer^{b,*}

^a Department of Electrical and Computer Engineering, University of California, San Diego, La Jolla, CA 92093, USA

^b School of Medicine, University of California, San Diego, La Jolla, CA 92093, USA

^c VA San Diego Healthcare System, San Diego, CA 92161, USA



ARTICLE INFO

Keywords:

Yeast secretion
Point-of-care diagnostics
Hepatitis C virus
Whole-cell biosensor
Electrochemical biosensor

ABSTRACT

Access to affordable and field deployable diagnostics are key barriers to the control and eradication of many endemic and emerging infectious diseases. While cost, accuracy, and usability have all improved in recent years, there remains a pressing need for even less expensive and more scalable technologies. To that end, we explored new methods to inexpensively produce and couple protein-based biosensing molecules (affinity reagents) with scalable electrochemical sensors. Previous whole-cell constructs resulted in confounding measurements in clinical testing due to significant cross-reactivity when probing for host-immune (antibody) response to infection. To address this, we developed two complimentary strategies based on either the release of surface displayed or secretion of fusion proteins. These dual affinity biosensing elements couple antibody recognition (using antigen) and sensor surface adhesion (using gold-binding peptide-GBP) to allow single-step reagent production, purification, and biosensor assembly. As a proof-of-concept, we developed Hepatitis C virus (HCV)-core antigen-GBP fusion proteins. These constructs were first tested and optimized for consistent surface adhesion then the assembled immunosensors were tested for cross-reactivity and evaluated for performance *in vitro*. We observed loss of function of the released reagents while secreted constructs performed well in *in vitro* testing with 2 orders of dynamic range, and a limit of detection of 32 nM. Finally, we validated the secreted platform with clinical isolates (n = 3) with statistically significant differentiation of positive vs. non-infected serum (p < 0.0001) demonstrating the ability to clearly distinguish HCV positive and negative clinical samples.

1. Introduction

Hepatitis C virus (HCV) is a positive sense, single-stranded RNA virus in the Flaviviridae family that is transmitted through blood transfusion, unsafe drug use, improperly sterilized medical devices, and unprotected intercourse. Exposure classically results in chronic infection and is present in over 70 million people globally, causing significant morbidity and mortality from cirrhosis, liver failure, and hepatocellular carcinoma (Chen and Morgan, 2006; Hepatitis C, n.d.). The World Health Organization (WHO) has set 2030 targets to reduce new infections by 90% and mortality by 65% from their 2015 levels (WHO | Combating hepatitis B and C to reach elimination by 2030, 2016). However, effective vaccine development against HCV is impeded by the high genetic heterogeneity and hence disease control is dependent on diagnosis, treatment, and cure using direct antiviral therapy, which is safe and highly effective (over 95%) for most patients (Doyle et al., 2013). As there is no animal reservoir (i.e., only humans can become

infected), curative therapy makes a “test-and-treat” strategy aimed at global HCV eradication feasible. Thus, identification of all HCV-infected persons is crucial to achieving this goal. While sensitive point-of-care (POC) screening is presently available (Fisher et al., 2015), diagnosis of HCV infection still poses a significant logistic and economic burden on healthcare systems in resource limited settings (Lemoine et al., 2013; Morgan et al., 2017), hence the impetus to develop ultra-low-cost POC reagents and testing platforms.

Currently, host antibody-directed platforms are used for primary screening and largely target anti HCV-core antigen due to its genetic conservation and direct correlation to viral RNA load (Barrera et al., 1995; Gretch, 1997; Kao et al., 1996; Park et al., 2010). To produce these diagnostic tests, affinity reagents (e.g., antigen, antibodies, aptamers, etc.) must be synthesized, purified, and coupled to biosensor surfaces. Choice of affinity molecule (e.g., HCV-core) as well as functionalization method are essential for diagnostic performance (Castillo et al., 2004). Current functionalization methods include physical

* Correspondence to: University of California, San Diego, 9500 Gilman Drive, La Jolla, CA 92093, USA

E-mail address: earonoffspencer@ucsd.edu (E. Aronoff-Spencer).

adsorption and chemical cross-linking, both of which are well described in the literature, but have disadvantages (e.g., partial denaturation, incorrectly oriented or sterically constrained protein deposition, etc.) leading to a loss of binding efficiency (Rusmini et al., 2007). While traditional affinity assay production methods have enabled wide-spread testing for as little as a few dollars per test, new technologies are needed that can bring costs down by another factor of ten or more while improving reagent stability and reliability.

To this end, whole-cell biosensors, membrane extracts, and fusion proteins have been studied and reported for biological sensing constructs (Grewal et al., 2014; Racek and Musil, 1987; Rawson et al., 1989; Shabani et al., 2008; Si et al., 2016; Su et al., 1986). These methods rely on cell-surface display of affinity molecules and address some of the disadvantages of classical manufactured platforms by presenting dense, oriented, and stable proteins. Importantly, these methods also reduce cost by streamlining protein production, purification, and sensor functionalization (Acosta-Rivero et al., 2002; Baumert et al., 1998; Harada et al., 1991; Madesis et al., 2010; Majeau et al., 2004). Immobilization is readily achieved by co-expression of fusion proteins with peptide sequences that are known to specifically bind to metals (Sarikaya et al., 2003; Stanley, 1997), oxides (Lee et al., 2002; Thai et al., 2004), or semiconductors (Gu et al., 2009; Peelle et al., 2005). Among these, gold binding peptide (GBP) is known to avidly bind metal surfaces with excellent surface retention over time (Heo et al., 2012). Thus, creating a fusion protein that consists of an affinity reagent (antibody or antigen) and GBP obviates the need for multi-step purification and immobilization procedures, enabling a single-step process (Zheng et al., 2010). Such constructs can be coupled with biosensors to facilitate low-cost POC-sensing systems thus freeing testing from centralized medical facilities (Sun et al., 2016a, 2016b). Many different biosensing modalities are possible such as optical (Hoa et al., 2007), electrochemical (Wang, 2006), magnetic (Hall et al., 2010), calorimetric (Zhang and Tadigadapa, 2004), etc. Each of these techniques has a unique set of advantages and disadvantages. We have focused on electrochemical sensors since they have been reported to have high sensitivity, can be manufactured cheaply at scale, and are easy to translate to POC applications without the need for complex, bulky optics. While these approaches point to potential advances in reagent production, they remain unproven in clinical settings (Cherf and Cochran, 2015; Du et al., 2005; Gray et al., 2012; Kahn et al., 2015, 2015; Qin et al., 2014; Slomovic et al., 2015; van Bloois et al., 2011).

In this paper we report a secreted dual-affinity fusion protein that combines HCV-core antigen with GBP repeats allowing single step purification and electrochemical assay functionalization directly from concentrated yeast supernatant. We benchmarked the system using

low-cost electrochemical sensing and, for the first time, demonstrate the use of such a construct to detect virus in clinical isolates. We chose yeast secretion of dual-affinity reagents as it combines high density fermentation with the ability for eukaryotic post-translational processing and removes the need for additional purification-only moieties such as His-6 (Lichty et al., 2005). In theory, this could provide higher yield and lower end-to-end cost than previously reported intra-cellular expression techniques. We also report a technique for releasing surface displayed fusion proteins, although we found that it is not appropriate for all constructs and unfortunately does not work with HCV. Our approaches to detect circulating anti-HCV-core antibody in human serum are shown in (Fig. 1).

2. Materials and methods

2.1. Construction of HCV-core:GBP yeast secretion vectors

The complete HCV-core gene was cloned by polymerase chain reaction (PCR) with forward and reverse primers consisting of NheI and BamHI, respectively from pCMV3010-HCV1, an HCV1 genome library constructed from a clinical sample. The PCR product was then restriction digested (NheI and BamHI), cleaned, and ligated into the pRS314 vector. The DNA sequence corresponding to GBP (sequence: MHGKT-QATSGTIQS) was cloned from template (Stanley, 1997) by PCR with both forward and reverse primers consisting of BamHI site. The PCR product was then digested with BamHI and inserted adjacent to HCV-core gene by ligation. The sequence of all vectors was confirmed by capillary population sequencing.

2.2. Transformation and induction of yeast secretion vectors

The constructed vectors were transformed into *S. cerevisiae* YVH10 strain from ATCC using the DSY yeast transformation kit (Dualsystems Biotech AG, #P01003) for display and secretion, respectively. The transformed HCV-core:GBP expressing yeast were then freshly streaked on SD + CAA selective media plates at 30 °C overnight. A fresh single colony was subsequently inoculated in 5 mL of SR + CAA media and incubated for 2 days at 30 °C, diluted to achieve 1 OD₆₀₀, and aliquoted in 1 mL batches. The expression was induced by inoculating 0.5 mL from 1 mL aliquots in 5 mL of S/Galactose and Raffinose + CAA media and incubated for 48 h at 20 °C. Preparation of media is described in the [Supplementary materials](#) for reference (Venkatesh et al., 2015).

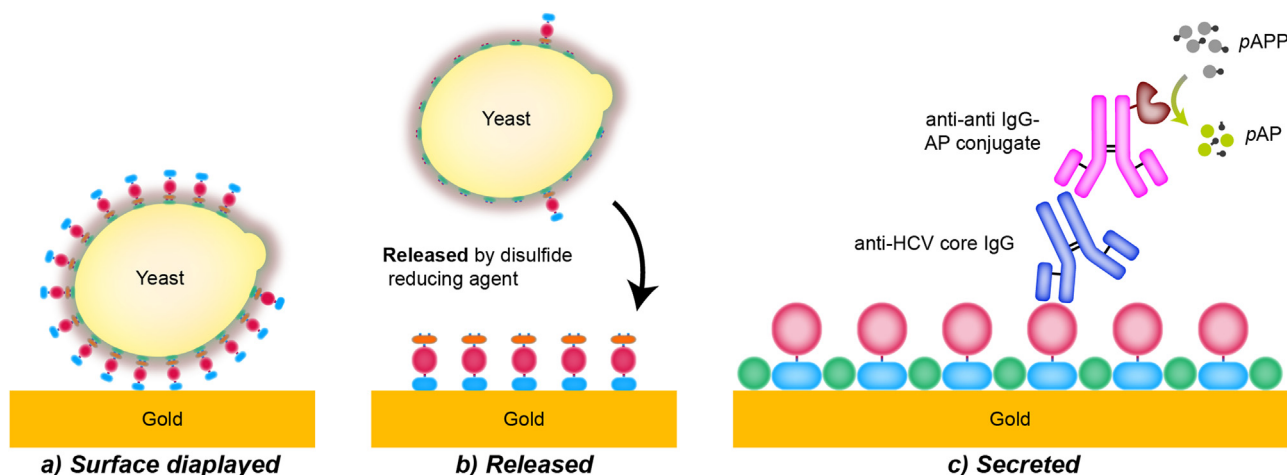


Fig. 1. Illustration showing HCV-core:GBP yeast fusion proteins bound to a gold electrode surface. Three strategies were developed using: a) whole-cell surface display, b) released fusion proteins, and c) secreted fusion proteins.

2.3. Fluorescent and immunochemical assay for yeast secretion validation

50 μ L cell-free galactose induced media containing the secreted HCV-core:GBP fusion protein was applied to a clean gold electrode (Dropsens, #DRP-250AT) (cleaning procedure described later) and incubated overnight at 4 °C. The electrode was then blocked with 50 μ L 2% Bovine Serum Albumin (BSA) in 1 \times PBS for 1 h. Two different anti HCV-core IgG were selected for separate experiments i.e., mouse monoclonal IgG (Santa Cruz Biotech, #sc-57800) and rabbit polyclonal IgG (Abcam, #ab58713). The primary IgG at desired concentration was incubated for 2 h at room temperature and washed once by rinsing 1 mL 1 \times PBS and air-blow dried. For fluorescent assays, mouse and rabbit primary antibodies were detected by Alexa Fluor 647 conjugated donkey anti-mouse IgG (Thermo Fischer, #A-31571) and goat anti-rabbit IgG (Thermo Fischer, #A-21244), respectively, incubated for 1 h, rinsed 3 \times with 1 mL 1 \times PBS, and air-blow dried. The electrode was then imaged by fluorescent microscopy with suitable filters. In the case of immunochemical assays, horseradish peroxidase (HRP)-conjugated donkey anti-mouse IgG (Abcam, #6820) and goat anti-rabbit IgG (Abcam, #ab6721) were used instead of Alexa Fluor 647. The immune complex was detected by adding 50 μ L 3,3',5,5'-Tetramethylbenzidine (TMB) substrate (Thermo Fischer, #34028) for 5 min and the enzymatic reaction was quenched by adding 10 μ L 2N sulfuric acid. The yellow colored solution was recovered from the electrode and measured for absorbance at 450 nm wavelength using a UV–Vis spectrophotometer.

2.4. Human serum samples

Healthy human AB serum free of HCV infection was procured from Omega Scientific (#HS-20). The patient samples used were obtained during routine clinical care and devoid of all personal identifying information.

2.5. Fluorescent immunoassay of clinical samples

100 μ L galactose induced yeast cells were centrifuged in 96-well plates and re-suspended in 50 μ L 1 \times PBS containing 1% BSA and incubated at room temperature for 30 min to pre-block the surface. 50 μ L of serially diluted deidentified clinical serum samples (undiluted, 1:20, and 1:200 dilutions) were individually added to the yeast cells and the plate was gently rocked for 2 h at room temperature. The yeast cells were then washed 4 \times with 50 μ L 1 \times PBS by centrifugation and re-suspension. The Alexa Fluor 488 conjugated donkey anti-human IgG (Abcam, #ab150073) was subsequently added and incubated for 1 h at room temperature followed by 4 \times wash with 50 μ L 1 \times PBS. Pellets were then re-suspended in 20 μ L 1 \times PBS and measured for fluorescence using a microtiter plate reader with suitable excitation and emission filters (Tecan F200).

2.6. Procedure for cleaning electrode

Prior to functionalizing the gold sensing surface, screen-printed gold electrodes (Dropsens, #DRP-250AT) were cleaned using a two-step procedure. First, organic residual curing ink (if any) was cleaned by placing the electrode in 50 mM KOH/H₂O₂ (3:1) solution for 10 min. The electrode was then cleaned by cyclic voltammetry (CV) in the presence of 50 mM H₂SO₄ to remove oxide layer from gold surface. A potential between −0.4 V to +1.4 V was swept at a rate of 100 mV/s for 12 cycles using a benchtop potentiostat (CH Instruments 750E).

2.7. Functionalization of gold surface with fusion proteins

Optimal surface functionalization was explored with various buffers (and strengths), varying incubation temperatures, durations, and starting amounts of cell supernatant to optimize protein binding to gold-surfaces (data not shown). Optimal conditions were noted with

freshly grown cells, TBS, and overnight loading at 4 °C. For this work, 50 μ L 1 OD₆₀₀ cells suspended in induction media or cell-free induction media containing secreted fusion protein was dropcast on a clean gold electrode surface and incubated overnight at 4 °C. The electrodes were then rinsed with 1 mL 1 \times TBS (Tris buffered saline pH 7.4), and only the electrodes with yeast cells were treated with 50 μ L 1% Sodium azide in 1 \times TBS for 90 min at room temperature and rinsed with 1 mL TBS. The sensor electrodes with both displayed and secreted were blocked with 1 \times TBS containing 2% BSA and 0.05% TWEEN-20 for 1 h at room temperature and rinsed with 1 mL TBS.

2.8. Electrochemical indirect ELISA

The functionalized electrode was incubated with 20 μ L of anti-HCV antibody derived from either mouse monoclonal IgG (Santa Cruz Biotech, #sc-57800) or rabbit polyclonal IgG (Abcam, #ab58713) for 2 h at room temperature and rinsed with 1 mL TBS. 20 μ L of Alkaline phosphatase (ALP) conjugated secondary IgG's from rabbit (Abcam, #ab6729) and goat (Abcam, #ab6722) targeted towards mouse IgG and rabbit IgG, respectively, were added and incubated for 1 h at room temperature. The electrode was then rinsed 3 \times with 1 mL TBS and air-blow dried. Immune complex formation was detected by adding 50 μ L substrate solution (100 mM glycine pH 10.4, 6 mM *p*-aminophenyl phosphate (*p*APP) (Santa Cruz Biotech, #sc-281392), 1 mM ZnCl₂ and 1 mM MgCl₂) to the electrode and incubated at 37 °C for 10 min. The conversion of *p*APP to *p*-aminophenol (*p*AP) by ALP was detected by cyclic voltammetry with a potential sweep between +0.3 V and −0.25 V at a rate of 25 mV/s for 10 cycles using CHI 750E or smart-phone-based potentiostat (Sun et al., 2016a, 2016b). The current vs. antibody concentration curve was fitted with 4-parameter logistic regression. Limit of detection (LOD) defined using the method described by Pry (Armbruster and Pry, 2008).

2.9. Serum pre-treatment

The serum was incubated with non-surface display yeast strain for 30 min at room temperature. After incubation, the cells were removed by centrifugation at 5000 RPM for 10 min and used for anti HCV-core IgG assay.

2.10. HCV-core:GBP fusion protein release

Yeast cells displaying HCV-core:GBP fusion protein were treated with 100 mM Dithiothreitol (DTT) at room temperature for 30 min and the released proteins were harvested by centrifugation at 5000 RPM for 5 min. The gold working electrode of the biosensor was then functionalized with the released Aga2:HCV-core:GBP fusion protein.

3. Results and discussion

3.1. Clinical assay with surface displayed HCV-core

We recently reported development and performed in vitro testing of an HCV biosensor using whole-cell yeast displaying HCV-core antigen:GBP as a primary affinity reagent to detect host antibody response (Aronoff-Spencer et al., 2016). We then tested these assays using sera from control and infected individuals; however, we obtained inconsistent results with no discernable difference ($p > 0.5$) between HCV positive and HCV negative samples (Fig. 2a). Notably, there was significantly elevated background signal (despite reducing the assay time from 10 min to 1 min) compared to testing in buffer solution. We hypothesized this background signal was due to non-specific binding of yeast-directed immune factors such as heterophile or Rheumatoid antibodies present in serum. To test this hypothesis, clinical samples were pre-treated by incubation with varying concentrations of yeast cells without HCV-core antigen to deplete such immune factors, and the

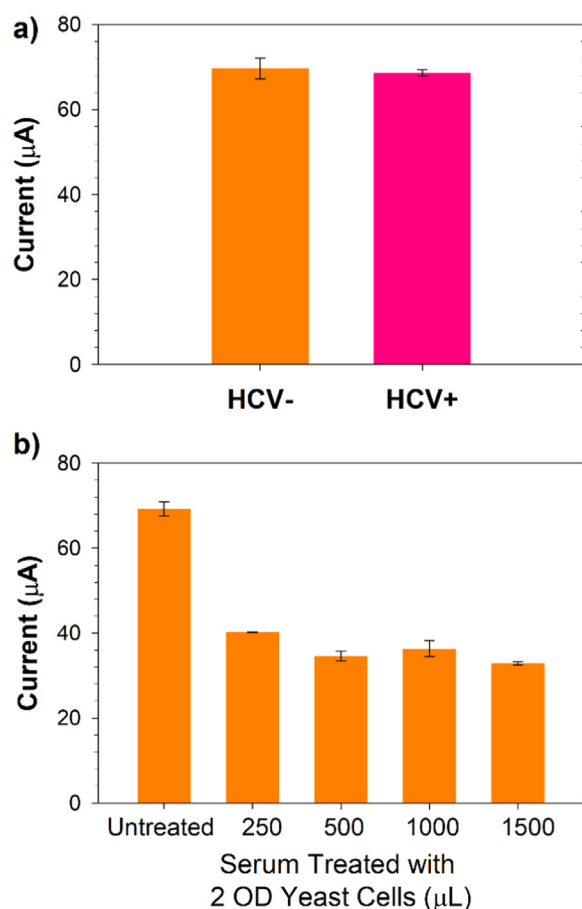


Fig. 2. Yeast antigen display-based anti HCV-core detection in human serum: a) False positive due to non-specific binding of human IgG to yeast surface antigens, and b) Reduction of non-specific binding by pre-absorbing human IgG using varying concentrations of yeast cells with no HCV-core display.

serum was assayed. While a significant difference in background ($2\text{--}3 \times$ reduction) was observed between untreated and pre-absorbed serum, the background signal remained too high for reproducible testing with clinical specimens (Fig. 2b). This highlights a potential drawback of whole-cell sensing of host immune response but is not an issue when antibody is displayed and is used for sensing of antigen in test specimens.

3.2. Expression and secretion of HCV-core from yeast

As serum pre-absorption failed to sufficiently reduce background binding, alternative methods such as release and secretion of the surface-displayed fusion protein were investigated. In whole-cell experiments, the surface-displayed HCV-core:GBP protein is bound by a peptide bond to Aga-2, which is linked by twin-disulfide bridges to Aga-1 and the yeast surface (Aronoff-Spencer et al., 2016). The displayed complex can thus be released by treating the cells with dithiothreitol (DTT) or other disulfide reducing agents. A complete anti HCV-core IgG detection assay was performed using this approach (Supplementary Fig. S1), yet no functional activity was observed, likely due to reduction of a highly conserved stabilizing disulfide bridge in the HCV-core antigen (Kushima et al., 2010). This observation is contrary to the functionally viable assay with released scFv capable of detecting HIV gp120 antigen (Supplementary Fig. S2) and emphasizes that the release of affinity reagents by disulfide reduction is not universally suitable but can work for certain proteins. As a final step to address non-specific binding, HCV-core:GBP fusion proteins were developed for yeast secretion to produce cell-free dual affinity reagents.

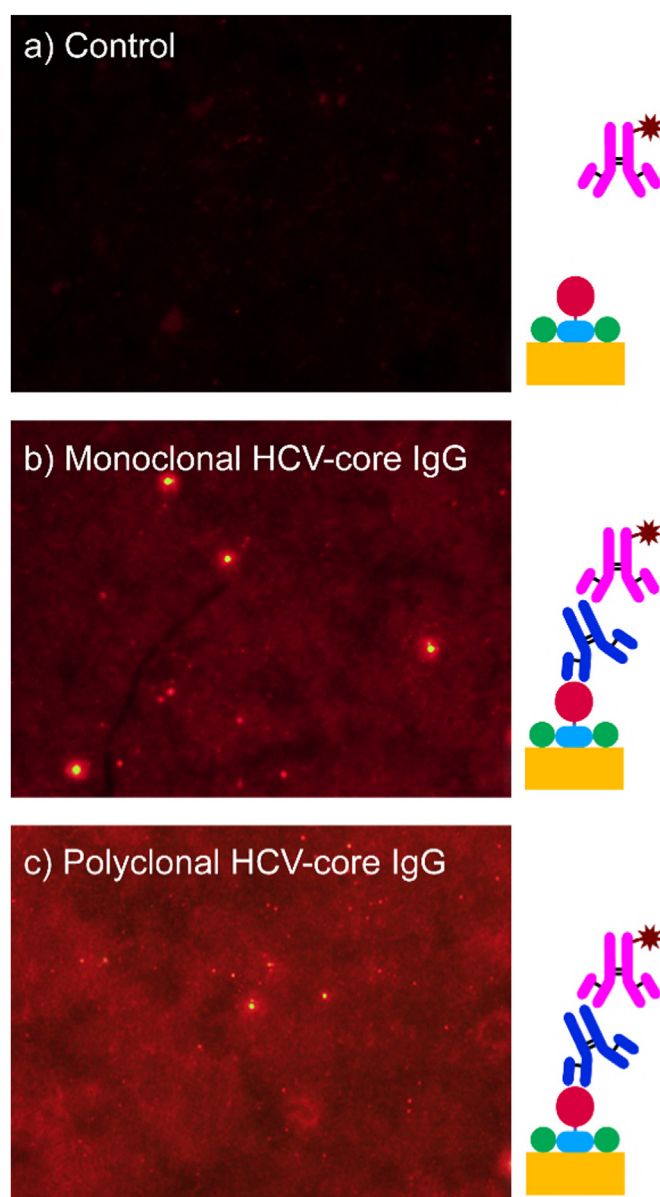


Fig. 3. Dense and specific binding of secreted affinity reagents to gold coated surface detected by fluorescent ELISA: a) No anti HCV-core IgG, b) Mouse monoclonal anti HCV-core IgG, and c) Rabbit polyclonal anti HCV-core IgG.

3.3. Validation of HCV-core affinity immuno-fluorescence assay

Cell-free secreted HCV-core:GBP fusion proteins were first tested for gold surface adduction and antibody binding. Fig. 3 depicts immuno-fluorescent assays of both surface and antibody binding, where Fig. 3a is a negative control (no anti HCV-core antibody was added to the electrode) and Fig. 3b,c had mouse monoclonal and rabbit polyclonal IgGs, respectively. The difference in red channel brightness is indicative of secreted HCV-core capture of anti HCV-core IgG. An increased fluorescence signal was observed with polyclonal antibody ($10 \times$ larger than the control) compared to monoclonal ($6 \times$ larger than the control) likely due to the presence of multiple epitope recognition sites in the HCV-core protein. It is worth noting that some of the visible bright spots are artifacts from the screen-printed gold surface and not due to immune-complex formation and were thus removed during image analysis.

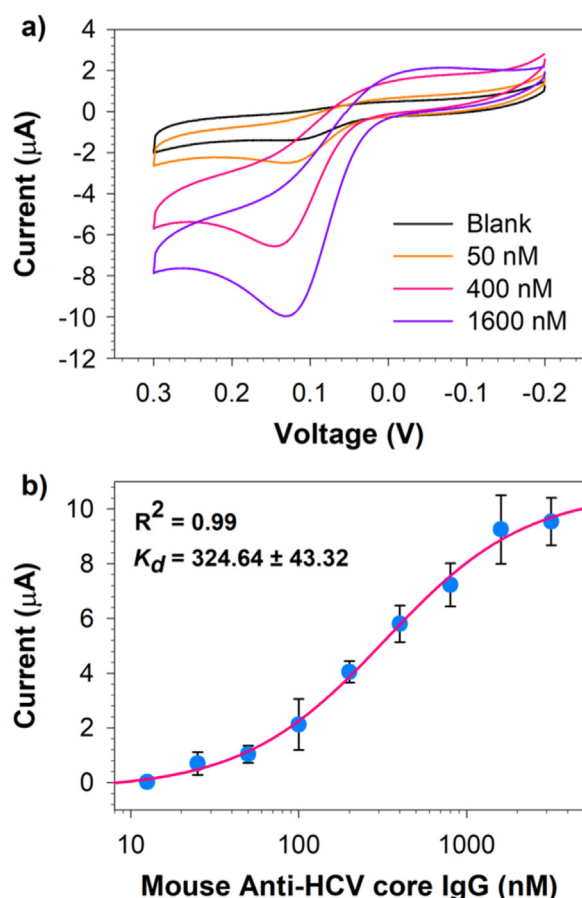


Fig. 4. Electrochemical ELISA for detection of anti-HCV core IgG: a) Voltammogram of selected mouse anti-HCV core IgG concentration, and b) Calibration curve showing detection of mouse monoclonal anti HCV-core IgG. The mean and standard deviation of all concentrations are from triplicates and fitted with 4-parameter logistic regression.

3.4. Development of electrochemical ELISA

After the affinities of secreted HCV-core fusion protein (to both gold surfaces and target antibody) were assessed by immunofluorescence, a sandwich electrochemical assay was developed. Calibration curves were generated in TBS from measured cyclic voltammograms (CVs) to assess assay parameters such as the limit of detection (LOD), dynamic range (DR), and dissociation constant (K_d) of the secreted HCV-core fusion protein functionalized SPEs to detect monoclonal anti HCV-core IgG (Fig. 4). Measurements with this construct proved to be robust, but demonstrated a higher LOD (32 nM), DR (32 nM–3.2 μM) and K_d (324.64 ± 43.32 nM) compared to their whole-cell equivalent constructs (Aronoff-Spencer et al., 2016). Raw data and fit parameters are reported in Supplementary Table S1. We hypothesize that this reduction in affinity is likely due to lower surface density of the new reagent, which could be remedied with a purification step. Another benefit of this cell-free construct is that the closer positioning of the HCV-core protein at the sensor surface enables other readout techniques such as electrochemical impedance spectroscopy (EIS) and surface plasmon resonance (SPR) that were not possible with the previous construct due to their large size.

3.5. Cross-reactivity of secreted HCV-core fusion protein

Specificity of the secreted HCV-core fusion protein was tested with a set of mouse antibodies (400 ng each) targeted against HIV-gp41, HIV-PVD, and human cytokeratin in TBS (Fig. 5). Electrochemical

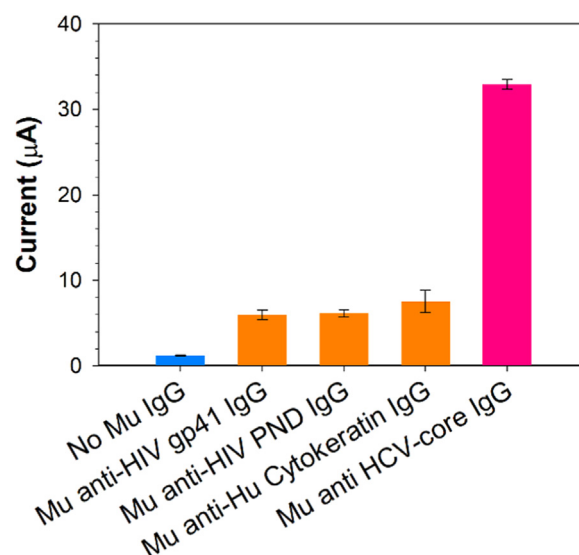


Fig. 5. Specificity of the secreted HCV-core:GBP fusion protein in discriminating non anti HCV-core mouse IgGs. HIV and Cytokeratin directed antibodies were selected as generic viral non-HCV and non-viral antigens.

measurements, labeled with ALP conjugated goat anti-mouse IgG, showed observable discrimination between anti HCV-core IgG and other non-specific IgGs from the same host. Statistically significant p -values were observed for all three non-specific mouse IgGs (anti-HIV gp41 IgG $p = 0.0001$, anti-HIV PND $p = 0.0001$, and anti Hu Cytokeratin $p = 0.0007$) compared to anti HCV-core IgG, demonstrating the ability of secreted HCV-core to discriminate non-anti HCV-core IgG. This data also demonstrates the high affinity towards human anti HCV-core IgG.

3.6. Performance of the HCV-core assay using clinical samples

The performance of the secreted fusion protein biosensor was tested using samples collected from anonymized human patients. HCV infected and negative sera were validated by gold-standard chemiluminescent immunoassay at ARUP laboratories, a national reference laboratory. Sera were then provided to the researchers blinded and measured using the secreted HCV-core:GBP fusion protein construct. Fig. 6 shows averaged data ($n = 3$) with significant differences in signal intensity between HCV positive samples from control and HCV negative patients. Blank measurements were taken with only the functionalized

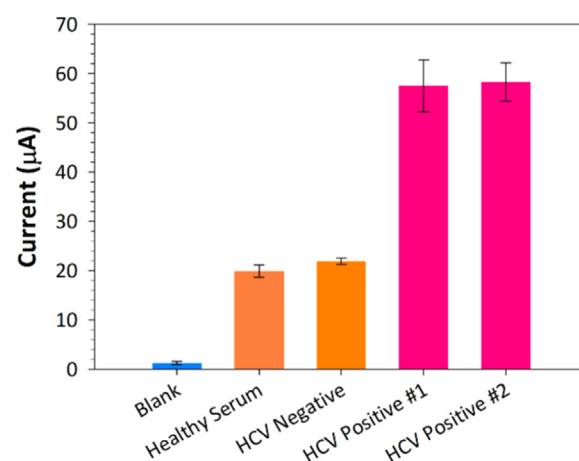


Fig. 6. Detection of anti HCV-core IgG in infected and control human serum samples ($n = 3$) by secreted HCV-core:GBP fusion protein.

biosensor and AP conjugated anti Human IgG, whereas the healthy human control was free of HCV infection. The HCV positive samples had significantly higher signal than the HCV negative samples ($p < 0.0001$) with no statistical difference between the HCV negative and control ($p = 0.0731$).

4. Conclusion

In this work, we developed and clinically validated a low-cost immunosensor using yeast-secreted affinity reagents non-covalently coupled to electrochemical detection circuitry. The work follows previously studied whole-cell antigen display systems that were found to have significantly elevated background. Two strategies were then developed to remove non-specific binding, either by releasing surface-displayed protein or, via yeast protein secretion pathways. We show that while released HCV core-proteins had loss of antigenicity due to disulfide disruption, secreted constructs retained avidity for both gold surfaces and directed antibodies, and could be produced with high yield. We then applied yeast supernatant with secreted proteins to directly functionalize gold-coated electrodes. These electrochemical immunosensors demonstrated sensitive and specific binding to core-directed polyclonal and monoclonal antibodies *in vitro*. Finally, we tested the platform with clinical isolates and found clear differentiation between infected and non-infected sera.

This study demonstrated limitations of whole-cell affinity reagents as immune probes due to potential non-specific and cross-reaction in human sera. We also showed that disulfide reduction as a method for release of surface displayed proteins can disrupt internal structure and reduce affinity in some cases. While the secreted constructs were shown to bind gold surfaces avidly, further characterization and optimization is needed. Likewise, while the limit of detection of 32 nM was sufficient to discern infection in a small group of clinical samples, the performance needs to be tested with greater sample numbers and at varying time points in hepatitis infection.

The above limitations point to future directions for work including validation and optimization of surface binding, exploration of various affinity tags and surface coatings, and further characterization and optimization of sensitivity and specificity of the assembled immunosensor in healthy and infected populations. Overall, we propose the combination of simple yeast-produced fusion protein reagents and smartphone-based sensors represents a promising opportunity for large-scale POC screening of medical and infectious diseases.

Acknowledgement

This research was funded in part by the UCSD Institute for Public Health (IPH) (Grant No.1UL1TR001442-01), UCSD Clinical and Translational Research Institute (UL1TR001442), Calit2 Strategic Research Opportunities (CSRO), and the UCSD Center for AIDS Research (CFAR) (P30 AI036214). CFAR is an NIH-funded program (P30 AI036214), which is supported by the following NIH Institutes and centers: NIAID, NCI, NIMH, NIDA, NICHD, NHLBI, NIA, NIGMS, and NIDDK. Special thanks to Dr. Chip Schooley for ongoing laboratory support.

Appendix A. Supporting information

Supplementary data associated with this article can be found in the online version at [doi:10.1016/j.bios.2018.07.026](https://doi.org/10.1016/j.bios.2018.07.026).

References

Acosta-Rivero, N., Musacchio, A., Lorenzo, L., Alvarez, C., Morales, J., 2002. Processing of the Hepatitis C virus precursor protein expressed in the methylotrophic yeast *Pichia pastoris*. *Biochem. Biophys. Res. Commun.* 295, 81–84. [https://doi.org/10.1016/S0006-291X\(02\)00635-6](https://doi.org/10.1016/S0006-291X(02)00635-6).

- Armbruster, D.A.L., Pry, T., 2008. Limit of blank, limit of detection and limit of quantitation. *Clin. Biochem. Rev. Suppl.* 1:549–52.
- Aronoff-Spencer, E., Venkatesh, A.G., Sun, A., Brickner, H., Looney, D., Hall, D.A., 2016. Detection of Hepatitis C core antibody by dual-affinity yeast chimera and smartphone-based electrochemical sensing. *Biosens. Bioelectron.* 86, 690–696. <https://doi.org/10.1016/j.bios.2016.07.023>.
- van Bloois, E., Winter, R.T., Kolmar, H., Fraaije, M.W., 2011. Decorating microbes: surface display of proteins on *Escherichia coli*. *Trends Biotechnol.* 29, 79–86. <https://doi.org/10.1016/j.tibtech.2010.11.003>.
- Barrera, J.M., Francis, B., Ercilla, G., Nelles, M., Achord, D., Darner, J., Lee, S.R., 1995. Improved detection of anti-HCV in post-transfusion hepatitis by a third-generation ELISA. *Vox Sang.* 68, 15–18.
- Baumert, T.F., Ito, S., Wong, D.T., Liang, T.J., 1998. Hepatitis C virus Structural proteins assemble into viruslike particles in insect cells. *J. Virol.* 72, 3827–3836.
- Castillo, J., Gáspár, S., Leth, S., Niculescu, M., Mortari, A., Bontidean, I., Soukharev, V., Dorneanu, S.A., Ryabov, A.D., Csöregi, E., 2004. Biosensors for life quality: design, development and applications. *Sens. Actuators B Chem.* 102, 179–194. <https://doi.org/10.1016/j.snb.2004.04.084>.
- Chen, S.L., Morgan, T.R., 2006. The natural history of Hepatitis C virus (HCV) infection. *Int. J. Med. Sci.* 3, 47–52.
- Cherf, G.M., Cochran, J.R., 2015. Applications of yeast surface display for protein engineering. *Methods Mol. Biol. Clifton NJ* 1319, 155–175. <https://doi.org/10.1007/978-1-4939-2748-7.8>.
- Doyle, J.S., Aspinall, E., Liew, D., Thompson, A.J., Hellard, M.E., 2013. Current and emerging antiviral treatments for hepatitis C infection. *Br. J. Clin. Pharmacol.* 75, 931–943. <https://doi.org/10.1111/j.1365-2125.2012.04419.x>.
- Du, C., Chan, W.C., McKeithan, T.W., Nickerson, K.W., 2005. Surface display of recombinant proteins on *Bacillus thuringiensis* spores. *Appl. Environ. Microbiol.* 71, 3337–3341. <https://doi.org/10.1128/AEM.71.6.3337-3341.2005>.
- Fisher, D.G., Hess, K.L., Erlyana, E., Reynolds, G.L., Cummins, C.A., Alonzo, T.A., 2015. Comparison of Rapid Point-of-Care Tests for Detection of Antibodies to Hepatitis C Virus. *Open Forum Infect. Dis.* 2, 1–6.
- Gray, S.A., Weigel, K.M., Ali, I.K.M., Lakey, A.A., Capalungan, J., Domingo, G.J., Cangelosi, G.A., 2012. Toward low-cost affinity reagents: lyophilized yeast-scFv probes specific for pathogen antigens. *PLoS One* 7, e32042. <https://doi.org/10.1371/journal.pone.0032042>.
- Gretch, D.R., 1997. Diagnostic tests for hepatitis C. *Hepatology Baltim. Md* 26, 435–475. <https://doi.org/10.1002/hep.510260708>.
- Grewal, Y.S., Shiddiky, M.J.A., Spadafora, L.J., Cangelosi, G.A., Trau, M., 2014. Nano-yeast-scFv probes on screen-printed gold electrodes for detection of *Entamoeba histolytica* antigens in a biological matrix. *Biosens. Bioelectron.* 55, 417–422. <https://doi.org/10.1016/j.bios.2013.12.043>.
- Gu, B., Park, T.J., Ahn, J.-H., Huang, X.-J., Lee, S.Y., Choi, Y.-K., 2009. Nanopag field-effect transistor biosensors for electrical detection of avian influenza. *Small* 5, 2407–2412. <https://doi.org/10.1002/sml.200900450>.
- Hall, D.A., Gaster, R.S., Lin, T., Osterfeld, S.J., Han, S., Murmann, B., Wang, S.X., 2010. GMR biosensor arrays: a system perspective. *Biosens. Bioelectron.* 25, 2051–2057.
- Harada, S., Watanabe, Y., Takeuchi, K., Suzuki, T., Katayama, T., Takebe, Y., Saito, I., Miyamura, T., 1991. Expression of processed core protein of hepatitis C virus in mammalian cells. *J. Virol.* 65, 3015–3021.
- Heo, N.S., Zheng, S., Yang, M., Lee, S.J., Lee, S.Y., Kim, H.-J., Park, J.Y., Lee, C.-S., Park, T.J., 2012. Label-free electrochemical diagnosis of viral antigens with genetically engineered fusion protein. *Sensors* 12, 10097–10108. <https://doi.org/10.3390/s120810097>.
- Hepatitis C. [WWW Document], n.d. World Health Organ. URL <http://www.who.int/news-room/fact-sheets/detail/hepatitis-c> (Accessed 26 April 2018).
- Hoa, X.D., Kirk, A.G., Tabrizian, M., 2007. Towards integrated and sensitive surface plasmon resonance biosensors: a review of recent progress. *Biosens. Bioelectron.* 23 (2), 151–160. Epub 2007 Jul 20.
- Wang, Joseph, 2006. Electrochemical biosensors: Towards point-of-care cancer diagnostics. *Biosens. Bioelectron.* 21 (10), 1887–1892.
- Kahn, M., Priddy, S., Estrada, M., Spadafora, L., Cangelosi, G.A., Domingo, G.J., 2015. Methodology for preservation of yeast-bound single chain fragment variable antibody affinity reagents. *J. Immunol. Methods* 427, 134–137. <https://doi.org/10.1016/j.jim.2015.11.003>.
- Kao, J.H., Lai, M.Y., Hwang, Y.T., Yang, P.M., Chen, P.J., Sheu, J.C., Wang, T.H., Hsu, H.C., Chen, D.S., 1996. Chronic hepatitis C without anti-hepatitis C antibodies by second-generation assay. A clinicopathologic study and demonstration of the usefulness of a third-generation assay. *Dig. Dis. Sci.* 41, 161–165.
- Kushima, Y., Wakita, T., Hijikata, M., 2010. A disulfide-bonded dimer of the core protein of Hepatitis C virus is important for virus-like particle production. *J. Virol.* 84, 9118–9127. <https://doi.org/10.1128/JVI.00402-10>.
- Lee, S.-W., Mao, C., Flynn, C.E., Belcher, A.M., 2002. Ordering of quantum dots using genetically engineered viruses. *Science* 296, 892–895. <https://doi.org/10.1126/science.1068054>.
- Lemoine, M., Nayagam, S., Thurst, M., 2013. Viral hepatitis in resource-limited countries and access to antiviral therapies: current and future challenges. *Future Virol.* 8, 371–380. <https://doi.org/10.2217/fvl.13.11>.
- Lichty, J.J., Malecki, J.L., Agnew, H.D., Michelson-Horowitz, D.J., Tan, S., 2005. Comparison of affinity tags for protein purification. *Protein Expr. Purif.* 41, 98–105. <https://doi.org/10.1016/j.pep.2005.01.019>.
- Madesis, P., Osathanunkul, M., Georgopoulou, U., Gisby, M.F., Mudd, E.A., Nianiou, I., Tsioura, P., Mavromara, P., Tsiftaris, A., Day, A., 2010. A hepatitis C virus core polypeptide expressed in chloroplasts detects anti-core antibodies in infected human sera. *J. Biotechnol.* 145, 377–386. <https://doi.org/10.1016/j.jbiotec.2009.12.001>.
- Majeau, N., Gagné, V., Boivin, A., Bolduc, M., Majeau, J.-A., Ouellet, D., Leclerc, D., 2004.

- The N-terminal half of the core protein of hepatitis C virus is sufficient for nucleocapsid formation. *J. Gen. Virol.* 85, 971–981. <https://doi.org/10.1099/vir.0.79775-0>.
- Morgan, J.R., Servidone, M., Easterbrook, P., Linas, B.P., 2017. Economic evaluation of HCV testing approaches in low and middle income countries. *BMC Infect. Dis.* 17, 697. <https://doi.org/10.1186/s12879-017-2779-9>.
- Park, Y., Lee, J.-H., Kim, B.S., Kim, D.Y., Han, K.-H., Kim, H.-S., 2010. New automated hepatitis C virus (HCV) core antigen assay as an alternative to real-time PCR for HCV RNA quantification. *J. Clin. Microbiol.* 48, 2253–2256. <https://doi.org/10.1128/JCM.01856-09>.
- Peelle, B.R., Krauland, E.M., Wittrup, K.D., Belcher, A.M., 2005. Probing the interface between biomolecules and inorganic materials using yeast surface display and genetic engineering. *Acta Biomater.* 1, 145–154. <https://doi.org/10.1016/j.actbio.2004.11.004>.
- Qin, J., Wang, X., Kong, J., Ma, C., Xu, P., 2014. Construction of a food-grade cell surface display system for *Lactobacillus casei*. *Microbiol. Res.* 169, 733–740. <https://doi.org/10.1016/j.micres.2014.02.001>.
- Racek, J., Musil, J., 1987. Biosensor for lactate determination in biological fluids. I. construction and properties of the biosensor. *Clin. Chim. Acta Int. J. Clin. Chem.* 162, 129–139.
- Rawson, D.M., Willmer, A.J., Turner, A.P., 1989. Whole-cell biosensors for environmental monitoring. *Biosensors* 4, 299–311.
- Rusmini, F., Zhong, Z., Feijen, J., 2007. Protein immobilization strategies for protein biochips. *Biomacromolecules* 8, 1775–1789. <https://doi.org/10.1021/bm061197b>.
- Sarikaya, M., Tamerler, C., Jen, A.K.-Y., Schulten, K., Baneyx, F., 2003. Molecular biomimetics: nanotechnology through biology. *Nat. Mater.* 2, 577–585. <https://doi.org/10.1038/nmat964>.
- Shabani, A., Zourob, M., Allain, B., Marquette, C.A., Lawrence, M.F., Mandeville, R., 2008. Bacteriophage-modified microarrays for the direct impedimetric detection of bacteria. *Anal. Chem.* 80, 9475–9482.
- Si, R., Yang, Y., Yu, Y., Han, S., Zhang, C., Sun, D., Zhai, D., Liu, X., Yong, Y., 2016. Wiring bacterial electron flow for sensitive whole-cell amperometric detection of riboflavin. *Anal. Chem.* 88, 11222–11228.
- Slomovic, S., Pardee, K., Collins, J.J., 2015. Synthetic biology devices for in vitro and in vivo diagnostics. *Proc. Natl. Acad. Sci. USA* 112, 14429–14435. <https://doi.org/10.1073/pnas.1508521112>.
- Stanley, B., 1997. Metal-recognition by repeating polypeptides. *Nat. Biotechnol.* 15, 269–272. <https://doi.org/10.1038/nbt0397-269>.
- Su, Y.C., Huang, J.H., Liu, M.L., 1986. A new biosensor for rapid BOD estimation by using immobilized growing cell beads. *Proc. Natl. Sci. Counc. Repub. China B* 10, 105–112.
- Sun, A., Venkatesh, A.G., Hall, D.A., 2016. A multi-technique reconfigurable electrochemical biosensor: enabling personal health monitoring in mobile devices. *IEEE Trans. Biomed. Circuits Syst.* 10, 945–954. <https://doi.org/10.1109/TBCAS.2016.2586504>.
- Sun, A.C., Yao, C., A.G., V., Hall, D.A., 2016. An efficient power harvesting mobile phone-based electrochemical biosensor for point-of-care health monitoring. *Sens. Actuators B Chem.* 235, 126–135. <https://doi.org/10.1016/j.snb.2016.05.010>.
- Thai, C.K., Dai, H., Sastry, M.S.R., Sarikaya, M., Schwartz, D.T., Baneyx, F., 2004. Identification and characterization of Cu₂O- and ZnO-binding polypeptides by *Escherichia coli* cell surface display: toward an understanding of metal oxide binding. *Biotechnol. Bioeng.* 87, 129–137. <https://doi.org/10.1002/bit.20149>.
- Venkatesh, A.G., Sun, A., Brickner, H., Looney, D., Hall, D.A., Aronoff-Spencer, E., 2015. Yeast dual-affinity biobricks: progress towards renewable whole-cell biosensors. *Biosens. Bioelectron.* 70, 462–468. <https://doi.org/10.1016/j.bios.2015.03.044>.
- WHO | Combating hepatitis B and C to reach elimination by 2030 [WWW Document], 2016. WHO. URL <<http://www.who.int/hepatitis/publications/hep-elimination-by-2030-brief/en/>> (Accessed 20 April 2016).
- Zhang, Y.L., Tadigadapa, S., 2004. Calorimetric biosensors with integrated microfluidic channels. *Biosens. Bioelectron.* 19 (12), 1733–1743.
- Zheng, S., Kim, D.-K., Park, T.J., Lee, S.J., Lee, S.Y., 2010. Label-free optical diagnosis of hepatitis B virus with genetically engineered fusion proteins. *Talanta* 82, 803–809. <https://doi.org/10.1016/j.talanta.2010.05.059>.